Lower Crustal Accretion and Reworking Beneath the North China Craton: Evidences from Granulite Xenoliths

22

Jianping Zheng, Ying Wei, Xianquan Ping, Huayun Tang, Yuping Su, Yilong Li, Zhiyong Li, and Bing Xia

Abstract

How has the Earth's deep continental crust evolved? Most of our knowledge is derived from surface exposures, but xenoliths carried in igneous rocks can be an important source of information. The North China Craton (NCC) is one of the oldest cratons in the world and Phanerozoic igneous rocks with abundant xenoliths are widespread, making it an ideal area to study the formation and evolution of continental crust. Abundant data of U–Pb ages and Hf isotopes in zircons were obtained for lower crustal xenoliths from over ten localities to constrain the history beneath the craton. The oldest components of the NCC may be ~4.0 Ga. The craton experienced complex accretion and reworking processes in its deep crust, accompanied by the formation and differentiation of the ancient continental nucleus. The small size of the NCC, compared with many other cratons worldwide, made it more susceptible to the effects of marginal subduction and collision with surrounding blocks. In the lower crust, the ancient components of the craton were reworked in Paleoarchean (3.80–3.65 Ga) time. The craton also experienced two important accretionary episodes, in the Neoarchean (2.8–2.5 Ga) and the Paleoproterozoic (2.3–1.8 Ga). Asthenospheric upwelling in Neoproterozoic time (0.6 Ga) locally modified the lower crust. Subduction and collision of the surrounding blocks, such as the Yangtze Craton, in Paleozoic and in early Mesozoic time also strongly modified the lower crust, especially along the cratonic margins. Accretion and modification of the lower crust during late Mesozoic–Paleogene were obvious due to the addition of depleted-mantle materials (underplating).

Keywords

Accretion and reworking • Lower crust • Xenoliths • North China Craton

22.1 Introduction

The primitive continental crust was derived from the differentiation of the early primitive mantle, and thus could be expected to show coupling with the subcontinental lithosphere mantle (SCLM) in terms of composition and age (Boyd 1989). However, subsequent interactions between mantle and crust, especially for ancient ones, can destroy such coupling and produce complex lithospheric structures. In the North China Craton (NCC), crustal rocks older than 3.6 Ga occur (Liu et al. 1992) and Paleozoic–Cenozoic igneous rocks erupted through the crust contain abundant xenoliths of lower crustal lithologies (e.g., Zhou et al. 1992; Fan et al. 1998; Zheng et al. 2004a), making this an ideal area to study the processes of formation and evolution of the continental crust.

In the northern part of the NCC, the oldest outcrops (i.e., Anshan Complex) are Paleoarchean (~3.8 Ga, Song et al.

J. Zheng (✉) · Y. Wei · X. Ping · H. Tang
Y. Su · Y. Li · Z. Li · B. Xia
State Key Laboratory of Geological Processes and Mineral Resources, School of Earth Sciences, China University of Geosciences, Wuhan, 430074, China
e-mail: jpzheng@cug.edu.cn

M. Zhai et al. (eds.), *Main Tectonic Events and Metallogeny of the North China Craton*, Springer Geology, DOI 10.1007/978-981-10-1064-4_22

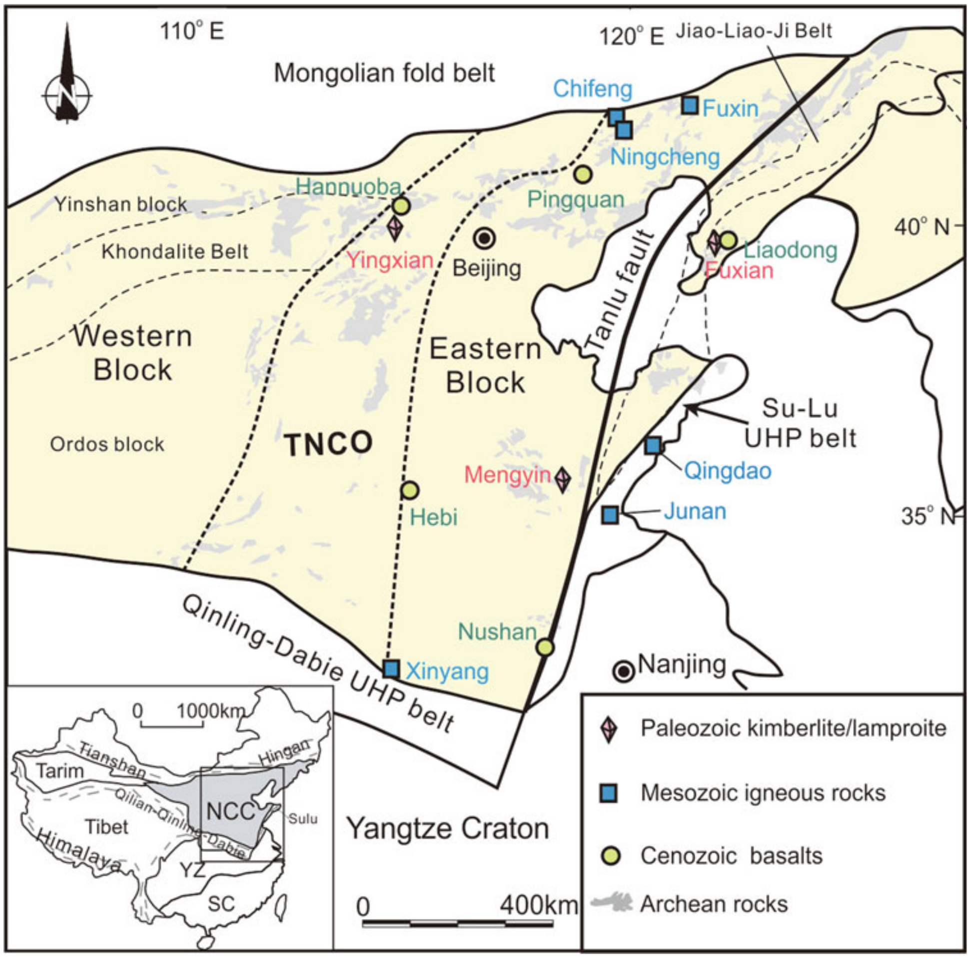

Fig. 22.1 Geological sketch map showing xenoliths localities for the Paleozoic (Mengyin, Fuxian, and Yingxian), Mesozoic (Chifeng, Ningcheng, Xinyang, Fuxin, Qingdao, and Junan), and Cenozoic (Pingquan, Liaodong, Hannuoba, Hebi, and Nushan) volcanic rocks within the North China Craton. *Abbreviations TNCO* the Trans-North China Orogen in the North China Craton (terminology of Zhao et al. 1999)

1996), whereas xenoliths of granulites in the nearby Cenozoic Hannuoba basalts indicate that the lowermost crust (>30 km deep) is mafic and Phanerozoic in age (470–47 Ma; Fan et al. 1998; Liu et al. 2001a; Wei et al. 2015; Wilde et al. 2003; Zheng et al. 2009a, 2012) whereas some of the middle lower crust (20–30 km depths) is intermediate and Paleoproterozoic in age (1.85 Ga; Zheng et al. 2004b). In contrast, in the southern part of the craton, the oldest outcrops (i.e., Taihua Complex) are Neoarchean (~2.85 Ga; Kröner et al. 1988), whereas garnet-free felsic granulite xenoliths from the Mesozoic Xinyang basaltic diatremes yield Paleoarchean U–Pb zircon ages (>3.65 Ga) for the upper part of the lower crust (Zheng et al. 2004a), showing that different deep-crustal structures exist in the different parts of the craton.

In this chapter, the synthetical investigation of zircon U–Pb ages and Hf isotopes for lower crustal xenoliths from northern to southern margin of the craton and the eastern block has been obtained to constrain the processes of accretion and reworking that have affected the deep continental lithosphere beneath the craton.

22.2 Spatial Distribution of Lower Crustal Xenoliths

The NCC is one of the major crustal blocks in the eastern part of the Eurasian continent. The Precambrian basement consists mainly of gneiss, migmatite, and high-pressure (HP) granulite facies rocks (Zhao et al. 2000; Zhai et al. 2001; Guo et al. 2002). The oldest upper crustal components, with ages >3.6 Ga, are found in the Caozhuang Group in Eastern Hebei Province and the Anshan Complex in Central Liaoning Province (Fig. 22.1; Liu et al. 1992; Song et al. 1996; Wan et al. 2005). The craton underwent a series of complex tectonic events in the late Archean and Paleoproterozoic (Zhai 2011; Kusky 2011). After assembly of the different micro-continental blocks (Zhao et al. 2000; Kusky and Li 2003) or cratonization (Zhai 2011) and subsequent rifting (Peng et al. 2008; Zhang et al. 2012b) in the Paleoproterozoic, the craton then was magmatically quiescent until the eruption of diamondiferous kimberlites in the middle Ordovician (Lu et al. 1998). Subduction along the southern margin of the NCC, accompanying its collision with the

Yangtze craton (YC), occurred in the Paleozoic (i.e., the Qinling belt in the western part; Yang et al. 2005) and in the early Mesozoic (i.e., the Sulu-Dabie belt in the eastern part; Li et al. 1993; Ye et al. 2000) to form the Qinling-Dabie-Sulu Orogenic Belt (Fig. 22.1), the world's largest UHP metamorphic belt (Liou et al. 2000; Ernst et al. 2007).

22.2.1 Xenoliths from the Paleozoic Igneous Rocks

The Paleozoic (457–480 Ma; Dobbs et al. 1994; Lu et al. 1998) Fuxian kimberlites and Yingxian lamproites (Fig. 22.1) erupted in southern Liaoning and northern Shanxi Provinces, respectively. In southern Liaoning Province, the Fuxian kimberlite pipes and dikes erupted through country rocks of Mesoproterozoic to Cambrian age. The lower crustal xenoliths in these kimberlites include garnet granulite, pyroxene amphibolite, metagabbro, and anorthosite (Zheng et al. 2004c, 2012). From the Fuxian kimberlite, garnet granulite is the most common xenolith type. These xenoliths are coarse-medium grained and reasonably fresh with well-developed granoblastic fabrics. The typical assemblage is garnet (22–69 %) + plagioclase + pyroxene ± K-feldspar ± quartz. Pyroxene amphibolite has a medium-fine grained assemblage of clinopyroxene + plagioclase + hornblende ± K-feldspar with well-developed granoblastic fabrics. Metagabbro is medium-fine grained with relict gabbroic microstructure. Some of the rocks contain up to 48 % K-feldspar, and should be regarded as syenites. Anorthosite consists of 94–95 % medium-coarse grained granoblastic plagioclase, and contains 2–3 % pseudomorphs of pyroxene and minor amounts of apatite and ilmenite.

From the Yingxian lamproites, some amphibolite xenoliths were collected. These amphibolites are generally round, from 8 to 10 cm in diameter. The xenoliths are homogeneous and consist of granoblastic assemblages of medium- to coarse-grained (1.8–3.5 mm) amphibole and plagioclase.

22.2.2 Xenoliths from the Mesozoic Igneous Rocks

Well-studied suites of deep-seated crustal xenoliths in the Mesozoic igneous rocks include: Chifeng and Ningcheng in Inner Mongolia (~221 Ma, Shao et al. 2012), Xinyang in southern Henan Province (~160 Ma, Zheng et al. 2008), Fuxin in northern Liaoning Province (100 Ma, Zhang and Zheng 2003), Qingdao (82 Ma; Zhang et al. 2008) and Junan (67 Ma; Ying et al. 2006) in southern Shandong Province (Fig. 22.1). They occur along the northern (Chifeng, Ningcheng and Fuxin) or southern (Xinyang, Qingdao and Junan) edges of the NCC.

The granulite xenoliths from the dioritic intrusion in Chifeng and Ningcheng are from 10 to 20 cm in diameter that can be divided into two-pyroxene granulite and Cpx-granulite and Hy-granulite based on the assemblage (Han and Shao 2000; Shao et al. 2000; Shao and Wei 2011). The granulites with granoblastic microstructure, mainly consist of hypersthene + diopside + plagioclase ± biotite ± quartz.

The xenoliths in Xinyang, at the intersection between the Trans-North China Orogen (TNCO, Zhao et al. 1999, 2000) [the Central Orogenic Belt of Kusky and Li (2003)] and the Qinling-Dabie Orogenic Belt (Fig. 22.1), include intermediate-felsic granulite, metagabbro, pyroxenite, high-pressure mafic granulite, and eclogite (Zheng et al. 2003, 2008). The intermediate granulite xenolith has a fine-grained granoblastic microstructure, and consists of plagioclase, garnet, clinopyroxene, and quartz. In contrast, the mafic granulite has less plagioclase and double garnet. Ilmenite and rutile are also appeared as accessory minerals in the mafic xenoliths. Metagabbro has a fine-grained granoblastic microstructure with relict gabbroic domains. Significantly, the pyroxenite and eclogite xenoliths in Xinyang have been identified as components of lower crust (Zheng et al. 2008). Pyroxenite consists mainly of garnet and diopside, and eclogite is composed primarily of coarse-grained garnet and omphacite.

Monzonite (Zheng et al. 2004d) and granulite (Tang et al. 2014; Ying et al. 2010) xenoliths can be found in the basalts from Fuxin and Junan, respectively. Monzonite is medium-fine grained microstructure, consists of plagioclase and alkali feldspar. Granulites are 1–15 cm in sizes with sub-angular to rounded shape. Among the constituent minerals, plagioclase has the highest abundance followed by orthopyroxene and clinopyroxene, quartz and Fe–Ti oxide are minor. Garnets can also be found in few granulites. Unlike Junan, the granulite xenoliths from Qingdao were captured by mafic dikes. The mineral assemblage is hypersthene, augite, and labradorite/bytownite. Garnet, amphibole, and mica are not observed (Zhang 2012 and references therein).

22.2.3 Xenoliths from the Cenozoic Basalts

Cenozoic basalts with lower crustal xenoliths/xenocrysts are widespread (Fig. 22.1), including: Liaodong (58 Ma) near the Paleozoic Fuxian kimberlites, Pingquan (45 Ma) in the Yanshan intercontinental orogen in the Eastern Block (EB), Hannuoba at the intersection between the Khondalite belt (Zhao et al. 2000) and the TNCO (22 Ma), Hebi (4 Ma) at the western edge of the EB, Nushan (2 Ma) at the southern end of the Tanlu Fault. Deep-seated crustal xenoliths in Pingquan (Zheng et al. 2012) and Hebi (Zheng et al. 2012) were reported rarely. The felsic and mafic granulites in the Pingquan Paleogene basalts are ellipsoidal ($6 \times 5 \times 4$ cm^3) or round

Table 22.1 Rock types of the deep-seated crustal xenoliths from Hannuoba

Xenolith type		Mineral assemblage (main)	Texture and structure	References
Felsic granulite		Pl + Af + Q ± Cpx ± Gt	Granoblastic; massive/foliated	Chen et al. (1998, 2001)
		Pl + Af + Q±Spn ± Gt		Zhang et al. (1998), Huang et al. (2001)
		Opx + Cpx + Pl ± Af		Liu et al. (2001a, b)
		Q + Pl + Gt ± Gr ± Sil ± Scp		Zheng et al. (2004b), Jiang and Guo (2010)
Intermediate granulite		Pl + Af + Q+Cpx ± Zr ± Ap	Granoblastic	Liu et al. (2001a, 2004)
		Pl + Opx + Cpx		
Mafic granulite	Two pyroxene-	Opx + Cpx + Pl ± Af ± Bi	granoblastic; massive/foliated	Fan and Liu (1996)
		Opx + Cpx + Pl ± Ol ± Ilm		Chen et al. (1998, 2001), Fan et al. (2005)
		Opx + Cpx + Pl ± Gt		Zhang et al. (1998), Huang et al. (2001)
		Cpx + Pl + Am + Gt		Liu et al. (2001a), Zhou et al. (2002)
	Noritic	Opx + Pl ± Q		Zheng et al. (2009a)
	Pl-riched	Pl + Opx + Cpx + Af		Jiang and Guo (2010)
	Gt-riched	Cpx + Gt + Pl ± Opx		Jiang et al. (2010), Du and Fan (2011)
Pyroxenite (some of granulite facies)	Clinopyroxenite	Cpx ± Sp ± Opx	Cumulatic; granoblastic	Fan et al. (2001, 2005)
	Gt-pyroxenite	Gt + Cpx ± Opx ± Ol ± Sp		Du and Fan (2011)
	Websterite	Opx + Cpx ± Sp		Jiang et al. (2010)
	Pl-pyroxenite	Pl + Cpx ± Opx ± Gt		

Abbreviations Pl plagioclase; *Af* alkali feldspar; *Q* quartz; *Cpx* clinopyroxene; *Gt* garnet; *Spn* sphene; *Opx* orthopyroxene; *Sil* sillimanite; *Scp* scapolite; *Zr* zircon; *Ap* apatite; *Bi* biotite; *Ilm* ilmenite; *Am* amphibole; *Sp* spinel

(~6.5 cm in diameter), and contain granoblastic assemblages of quartz + plagioclase + K-felspar and plagioclase + orthopyroxene + clinopyroxene, respectively (Zheng et al. 2012). The felsic granulite and amphibolite in Hebi are ellipsoidal, from 3 to 7 cm, with granoblastic structure, and composed of quartz + plagioclase + K-feldspar and amphibole + plagioclase, respectively (Zheng et al. 2012). However, there are much more abundant of lower crustal xenoliths in Nushan and Hannuoba. In Nushan, the xenoliths include felsic-intermediate and mafic granulite, granitic gneiss, and charnockite (Zhou et al. 1992; Huang et al. 2003, 2004; Zheng et al. 2012). The felsic granulite has granoblastic microstructure, consists of plagioclase + quartz ± diopside ± K-feldspar ± Fe–Ti oxide. The assemblages of granitic gneiss and charnockite are plagioclase + quartz + hypersthene and plagioclase + quartz + K-feldspar, respectively. The mafic granulites are with or without garnet, both typical of two-pyroxene granulites, and predominantly composed of orthopyroxene, clinopyroxene and plagioclase with subordinate amount of quartz and Fe–Ti oxides. All the mafic xenoliths are characterized by foliated structure. The lithological characteristics of the variety of xenoliths from Hannuoba are listed in Table 22.1, include felsic-intermediate granulite, mafic granulite with or without garnet, and some pyroxenite xenoliths that from the crust–mantle transitional zone.

22.3 Zircon U–Pb and Hf-isotope Systematics of the NCC Lower Crust

22.3.1 Lower Crustal Xenoliths/Xenocrysts in the Paleozoic Volcanic Rocks

Mafic xenoliths from the **Fuxian** kimberlites are mainly garnet granulite, with minor pyroxene amphibolite and metagabbro (Zheng et al. 2004c). U–Pb dating of zircons from four granulites reveals multiple age populations, recording several episodes of magmatic intrusion and subsequent metamorphic recrystallization. Concordant ages and upper intercept ages, interpreted as minimum estimates for the time of magmatic crystallization, range from 2620 to 2430 Ma in three granulites, two amphibolites, and two metagabbros. Lower intercept ages, represented by near-concordant zircons, are interpreted as reflecting metamorphic recrystallisation, and

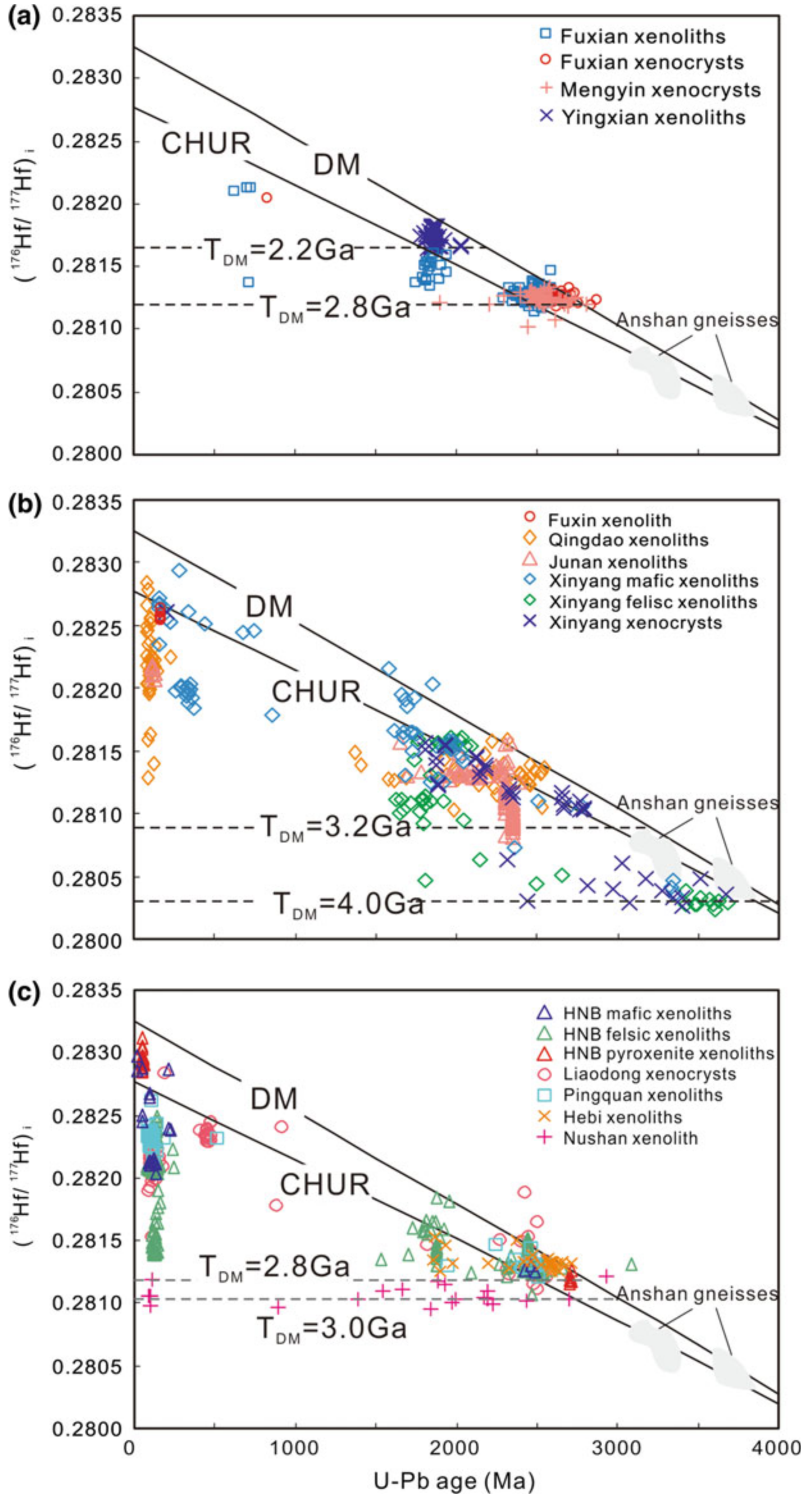

Fig. 22.2 ^{176}Hf/^{177}Hf versus U–Pb age for zircons from lower crustal xenoliths. **a** Fuxian xenolith and xenocryst: mafic xenoliths (Zheng et al. 2004c) and xenocrysts (Zheng et al. 2009b); Mengyin xenocrysts (Zheng et al. 2009b); Yingxian xenolith (Zheng et al. 2012). **b** Xinyang mafic xenoliths, felsic xenoliths, and xenocrysts (Zheng et al. 2004a, 2008); Fuxin Monzonite (Zheng et al. 2004d) and Junan granulite xenoliths (Ying et al. 2010; Tang et al. 2014); Qingdao mafic granulite xenoliths (Zhang 2012). **c** Felsic granulites from Pingquan (Zheng et al. 2004d, 2012) and from Nushan and Hebi (Zheng et al. 2012); Liaodong xenocrysts (Zhang et al. 2012b). Hannuoba xenoliths (Zheng et al. 2004b, 2009a; Jiang and Guo 2010; Jiang et al. 2010, 2011; Wei et al. 2015). *Other data sources* Anshan gneiss, Wu et al. (2008)

range from 1927 to 1852 Ma. One granulite contains two metamorphic zircon populations, dated at 1927 ± 55 Ma and 600–700 Ma (Zheng et al. 2004c). Zircon concentrates from the kimberlites give similar U–Pb ages to the mafic xenoliths, suggesting that these zircons are xenocrysts derived from the disaggregation of the xenoliths in the magma (Zheng et al. 2009b). Hf isotopic analyses of zircons show a range in $^{176}Hf/^{177}Hf$ from 0.281163 to 0.282139, corresponding to a range of ε_{Hf} from −37.4 to +11.4. The relationship between $^{207}Pb/^{206}Pb$ age and ε_{Hf} (Fig. 22.2a) of the zircons suggests that the mafic xenoliths were the products of basaltic underplating, with melts derived from a depleted mantle in Neoarchean time (2.8–2.5 Ga). The Paleoproterozoic metamorphic ages, accompanied by lower ε_{Hf}, indicate an important thermal event in the lower crust, corresponding to the timing of collision between the EB and WB that led to the final assembly of the NCC at ~1.85 Ga (Zhao et al. 2000) and its incorporation into the Columbia supercontinent (Kusky et al. 2007; Zhai 2011). The growth of metamorphic zircon at ~600 Ma may be related to an asthenospheric upwelling in Neoproterozoic time, which caused crustal uplift that is documented by a regional disconformity across the NCC (Zheng et al. 2004c).

Zircon xenocrysts from the **Mengyin** diamondiferous kimberlites have been used to probe the deep crust; no intact lower crustal xenoliths have been found. Based on detailed studies of external forms and internal structures, these zircons can be roughly divided into magmatic and metamorphic populations. The trace-element affinities of the igneous zircons vary widely from mafic, through intermediate, to felsic rocks with minor populations similar to zircons from carbonatite and syenite. Isotopic analysis of the U–Pb and Lu–Hf systems reveals that all zircons, regardless of their chemical affinities, have similar formation ages (2.7–2.5 Ga) and juvenile Hf isotopes, giving similar depleted-mantle model ages (T_{DM} = 2.8–2.7 Ga). These ages are also similar to those of zircons in mafic granulite xenoliths (Zheng et al. 2004c) and xenocrysts (Zheng et al. 2009b) from the Fuxian kimberlites (Fig. 22.2a), implying that the lower crust was similar beneath the Mengyin and Fuxian areas. Both have Neoarchean cratonic crust, but the latter experienced stronger thermal modification in Proterozoic time (Zheng et al. 2009b). However, the horizontal distribution of the Hf-isotope data in Fig. 22.2a reflects Pb loss without disturbance of the Hf-isotope composition, and does suggest that a thermal event also affected the Mengyin lower crust some time after 2.5 Ga.

Zircons from amphibolite xenoliths from the **Yingxian** lamproites are metamorphic with low Th/U. More than 95 % of the grains are concordant and give $^{207}Pb/^{206}Pb$ ages of 1.85 Ga and positive ε_{Hf}, showing addition of material derived from the depleted mantle during Paleoproterozoic time (2.2–1.85 Ga, Fig. 22.2a).

22.3.2 Lower Crustal Xenoliths in the Mesozoic Rocks

Zheng et al. (2004d) reported the U–Pb ages, Hf isotopes, and trace elements of zircons from two monzonite xenoliths from the **Fuxin** alkalic basalts (~100 Ma), and discussed the crust–mantle interaction that occurred in the Yanshanian intracontinental orogenic belt. The zircons show uniform U–Pb ages (169 ± 3 Ma) and have ε_{Hf} close to zero (Fig. 22.2b), indicating reworking of the lower crust beneath the Yanliao area during middle Jurassic time.

Ying et al. (2010) and Tang et al. (2014) reported geochronological and geochemical data for granulite xenoliths from a late Cretaceous basaltic breccia dike in **Junan**. The data reveal that the protolith of these xenoliths was formed around 2.3 Ga ago (Fig. 22.2b), probably by the remelting of >3.0 Ga crustal materials and mixing of the magmas with juvenile material. The lower crust beneath Junan that respected by these xenoliths has also experienced modification or metamorphism at 1.8–2.0 Ga and possibly Phanerozoic thermal events (Tang et al. 2014).

Zircon U–Pb geochronology and Hf isotope demonstrate that the lower crust lithologies beneath the **Qingdao** region formed at ~2.5 Ga and recorded an event without any signature for juvenile material input at 2.0 Ga. The peak ages (120 and 91 Ma) of magmatic underplating were also reported in this region (Zhang 2012).

The petrological and geochemical data from the **Xinyang** xenoliths show that the crust in this area is temporally and compositionally zoned: exposed rocks up to ca 2.85 Ga old (Kröner et al. 1988) are underlain by felsic granulites and rare pyroxenites with zircon ages of 3.6–3.4 Ga (to ca 30 km depth) (Zheng et al. 2004a). The Hf-isotope data indicate that the felsic granulites were derived from the remelting of crustal materials at least 4 Ga in age, older than the oldest known outcrops (Anshan gneisses) in the northern NCC (Fig. 22.2b). Deeper (ca 30–45 km) part of the lower crust consist of felsic to high-pressure mafic granulites and metagabbros, which give Paleoproterozoic (2.0–1.8 Ga) zircon ages similar to those from the Yingxian lamproites (Fig. 22.2a). These data show the significance of underplating and vertical crustal growth in the Paleoproterozoic, perhaps in response to the amalgamation of the Columbia supercontinent (Zhao et al. 2000; Kusky et al. 2007) and the final cratonization of the NCC (Zhai 2011). The wide spread of the Hf-isotope data at 2.0–1.8 Ga, as well as the wide spread of ages in zircons with similar Hf-isotope data, also indicate that both juvenile additions and reworking of older (3.8–3.0 Ga) crustal rocks were involved in this important event. Zircons with 440–260 Ma ages are found in eclogite xenoliths, showing the strong reworking of the deeper part of the lower crust in the Paleozoic in the early Mesozoic. This reworking may reflect the subduction and collision of the YC.

22.3.3 Lower Crustal Xenoliths in the Cenozoic Basalts

Zircon U–Pb dating, Hf isotopes and trace element data are available for xenoliths from the **Pingquan** alkali basalts, including one felsic granulite (Zheng et al. 2012), one mafic granulite (Zheng et al. 2012), and two monzonites (Zheng et al. 2004d). All the Neoarchean-early Paleoproterozoic zircons in the felsic granulite give positive ε_{Hf} (+0.8 to +8.4) and T_{DM} = 2.8–2.4 Ga, suggesting the addition of newly accreted materials in the lower crust at that time. This lower crust was again reworked in the middle Paleoproterozoic (1950 Ma). The ε_{Hf} values of the late Mesozoic zircons in both the felsic and mafic granulite xenoliths are negative (−20.8 to −8.9), suggesting the underplating of mafic magmas and assimilation of the older crustal components (Fig. 22.2c). In the monzonite, more than 95 % of the zircons give ages of 107 ± 10 Ma, except for two at 2491 and 513 Ma. The wide range of Hf model ages (0.89–2.56 Ga) in the monzonite zircons suggests the involvement of old crust in their petrogenesis, recording the reworking of Archean lower crust in late Mesozoic time.

The estimates of temperature and average pressure of the deep-seated crustal xenoliths from **Hannuoba** show that they were from different depths of the lower crust. Wei et al. (2015) proposed a three-layered structure of the lower crust beneath Hannuoba and showed that the felsic-mafic granulites comprise the upper lower crust (24–33 & 33–38 km) and the mafic products of basaltic underplating exist in the lower part (38–42 km). An updated compilation of zircon U–Pb ages from the deep-seated xenoliths carried by the Hannuoba basalts shows a large range from 45 to 534 Ma, with clusters at 45–47 Ma, 80–140 Ma, ∼220 Ma and others (Fig. 22.2c), reflecting multistage accretion and reworking of the lower crust during Phanerozoic time (Menzies et al. 2007; Zhu et al. 2011). The most ancient zircons with age of 2715 Ma are recorded by a pyroxenite xenolith and it has the similar Hf T_{DM} ages (2.7–2.8) to imply a major accretion event (Jiang et al. 2010). In comparison, many ∼2.5 Ga zircons from granulite xenoliths in Hannuoba have varied ε_{Hf}, distributed between the DM and CHUR evolution lines, which are considered to indicate significant reworking of 2.8–2.7 Ga continental crust accompanied by the growth of juvenile crust material (Wu et al. 2005; Zheng et al. 2009a; Jiang et al. 2010). A less important episode at 1.9–1.8 Ga is marked by some felsic granulites, coincided with the collision between the eastern and western blocks of the craton (Zhao et al. 2000). Zheng et al. (2004b) found that the intermediate granulite xenoliths from this locality contain no zircons younger than 1.73 Ga, suggesting considerable chemical and isotopic heterogeneity in the lower crust (Zhou et al. 2002). Fan et al. (1998) first provided concordant $^{206}Pb/^{238}U$ ages of 140–120 Ma for zircons in a Hannuoba mafic granulite, which was interpreted as the product of basaltic underplating in late Mesozoic (Liu et al. 2001a). Wilde et al. (2003) considered the Mesozoic crust–mantle interaction to be a consequence of the dispersal of Gondwanaland and the accretion of Asia, with a peak of activity around 180–80 Ma. Zheng et al. (2009a) reported the U–Pb and Hf isotope systematics of zircons, of five mafic xenoliths (granulites and pyroxenites) from the basalts. Most zircons in these lower crustal xenoliths give Paleogene (44.5–47.3 Ma) U–Pb ages which marked the event of basaltic underplating and fractionation (cumulates) with assimilation of some older intermediate crustal components; minor populations have Early Mesozoic (220–210 Ma), Late Mesozoic (90 Ma), and Neogene (14 Ma) ages. The Paleogene underplating corresponds in time to lithosphere-scale extension in the NCC, leading to the widespread formation of sedimentary basins (Ren et al. 2002). Most Paleogene zircons have positive ε_{Hf} (up to +13.2) with uniform T_{DM} (0.46–0.50 Ga), whereas most Mesozoic zircons have negative ε_{Hf}; this evolution suggests a temporal decrease in the degree of crustal assimilation during the extension of the lithosphere.

Most zircons in two deep-crustal xenoliths from **Hebi**, a felsic granulite, and an amphibolite, yield concordant $^{207}Pb/^{206}Pb$ age of 2.6 Ga and give T_{DM} = 2.7–2.6 Ga, showing the accretion of juvenile crust in Neoarchean time (Fig. 22.2c), similar to the thermal events recorded beneath Fuxian and Mengyin (see above and Fig. 22.2a).

Zhou et al. (1992) first reported the finding of granulite xenoliths in the **Nushan** basalts, and argued that they were derived from the ancient lower crust. Xu et al. (1998) combined the mineral chemistry of the granulite and peridotite xenoliths to construct an elevated geotherm beneath the area in Cenozoic time. Huang et al. (2003) proposed the existence of lower crust with early Paleozoic ages, based on the zircon geochronology of granulite xenoliths. Using the

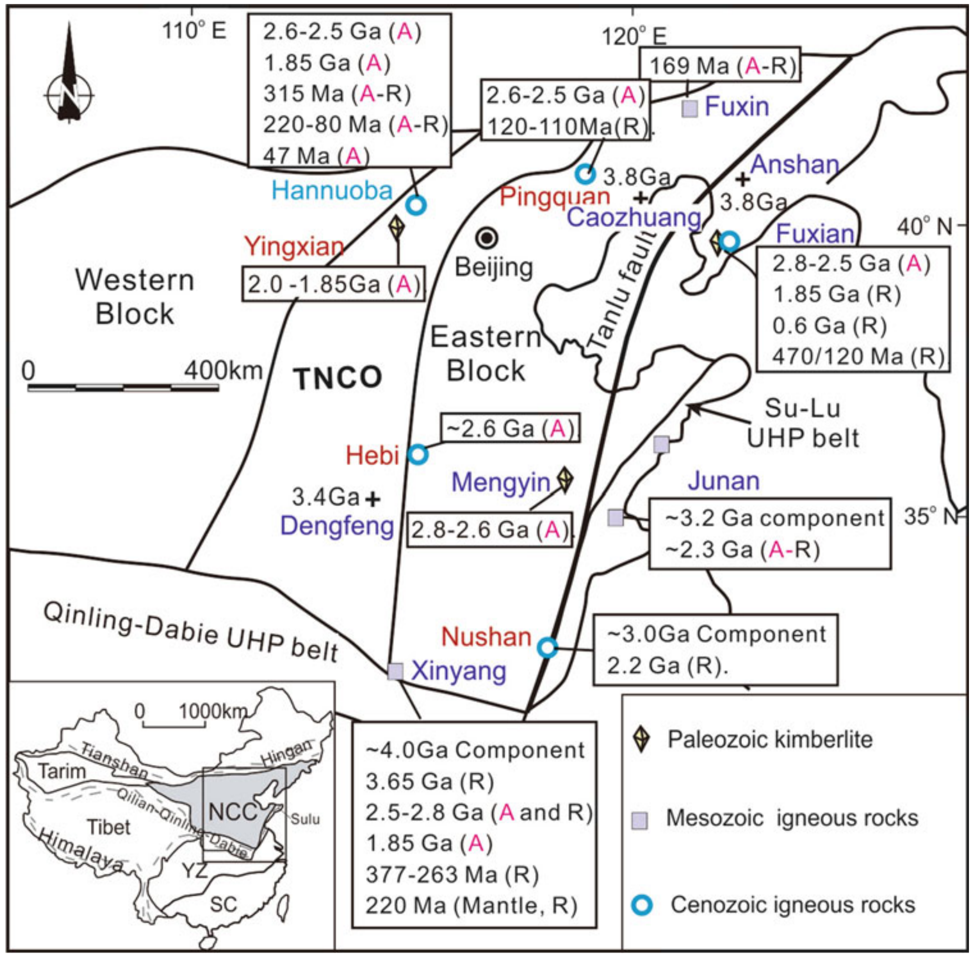

Fig. 22.3 Integration of accretion (*A*) and reworking (*R*) of the lower crust beneath the NCC recorded by xenoliths/xenocrysts. Original data sources are the same as Fig. 22.2. *Other data sources* Anshan, ~3.8 Ga outcrop, Song et al. (1996), Caozhuang, ~3.8 Ga outcrop, Liu et al. (1992). *Abbreviations TNCO* the Trans-North China Orogen in the North China Craton (terminology of Zhao et al. 1999)

geochemistry of the granulite xenoliths, Yu et al. (2003) tried to define different lower crustal characteristics between the NCC and the YC, though this interpretation was challenged. As described above, zircons from a felsic granulite have similar T_{DM} (3.0 Ga), and give an upper intercept age of 2.2 Ga and a lower intercept age of 49 ± 48 Ma. These zircons record the existence of >3.0 Ga components (Fig. 22.2c) and repeated lower crustal reworking in this area from at least 2.2 Ga to Cenozoic time.

Zhang et al. (2011) recently reported U–Pb and Hf-isotope analyses of zircon xenocrysts from the Cenozoic **Liaodong** basalts in southern Liaoning Province, near the Paleozoic Fuxian kimberlites. Three zircon populations were identified: Neoarchean (2.5 Ga), Paleozoic (mean 462 Ma), and Mesozoic (mean 120 Ma). The Precambrian grains have T_{DM} = 2.8–2.7 Ga, similar to the mafic granulite xenoliths (and their xenocrysts) from the Fuxian kimberlites (Zheng et al. 2004c, 2009b). The Phanerozoic (462 and 120 Ma) zircons have $\varepsilon_{Hf} = -26$ to -16, which imply some reworking of the Archean basement during later magmatic events (Fig. 22.2c).

22.4 Formation and Evolution of the North China Lower Crust

22.4.1 Eoarchean (~4.0 Ga) Components in the Lower Crust

The oldest rocks that outcrop in the NCC occur at Caozhuang in eastern Hebei and Anshan in central Liaoning Provinces. In Caozhuang, one-fourth of the zircons from an Archean metaquartzite have concordant U–Pb ages between 3.8 and 3.85 Ga (Liu et al. 1992); the zircons are interpreted as detritus derived from a terrain containing Eoarchean rocks. In Anshan, some zircons from sheared gneisses have concordant U–Pb ages with a weighted mean $^{207}Pb/^{206}Pb$ age of 3804 Ma, interpreted as the formation time of the protolith of the gneisses (Liu et al. 1992), which experienced episodic crustal reworking from the Archean to the Paleoproterozoic (Song et al. 1996; Wan et al. 2005).

The oldest zircons in the lower crustal xenoliths of the NCC were reported from Xinyang, at the southern margin of the craton (Fig. 22.1). These zircons in the felsic granulite xenoliths have a nearly concordant age as old as 3687 Ma (Zheng et al. 2004a). They also define a U–Pb discordia line with an upper intercept age of 3624 ± 69 Ma and a lower intercept age of 1793 ± 91 Ma, suggesting that they formed at ca ~3.6 Ga and suffered Pb loss at ca ~1.8 Ga. These zircons have a large range of Hf isotope compositions (ε_{Hf} = −41 to +4) with the negative εHf values observed for older (~3.6 Ga) zircons and the less negative to weakly positive ε_{Hf} values for younger (~1.8 Ga) grains; they produce two peaks in T_{DM} ages at ca 2.3 Ga and up to 4.0 Ga. All these age constraints and the Hf isotopes demonstrate that these granulite xenoliths formed in the Archean (3.6 Ga) and the remnants of the lower crust as represented by these xenoliths, i.e., the protolith of the melt from which the 3.6 Ga zircons crystallized, initially formed in the Eoarchean, as early as 4.0 Ga ago (see Xinyang in Fig. 22.3).

22.4.2 Neoarchean (2.8–2.5 Ga) Accretion and Reworking of the Lower Crust

The large dataset on zircon U–Pb ages demonstrates that the metamorphic terrains of the EB of the NCC, predominantly composed of TTG gneisses, formed in the late Neoarchean (Zhai et al. 2007; Geng et al. 2012). Minor supracrustal rocks are also present as bands, pods and enclaves within the TTG gneisses, such as metamorphosed mafic volcanics, sediments and banded iron formations (BIF). For example, in western Shandong Province, metamorphic rocks are exposed in the early Neoarchean (2.8–2.65 Ga) metamorphic volcano-sedimentary formations of the Taishan Complex and are strongly deformed together with the TTG gneisses (2.75–2.65 Ga; Jahn et al. 1988). The greenstone belt in the Complex, consisting of an assemblage of komatiites and pillow basalts, is also 2700–2800 Ma in age (Polat et al. 2006). The belt was intruded by gabbros, diorites, and high-Al TTG plutons and metamorphosed under amphibolite facies conditions at about 2700–2600 Ma (Wan et al. 2005). This activity has been interpreted as the product of a mantle plume–craton interaction (Polat et al. 2006). The western block (WB) (Fig. 22.1) is composed of the Ordos block, the khondalite belt and the Yinshan block (Zhao et al. 2000; Santosh et al. 2007). Recent studies have identified the khondalite belt as a collisional suture between the Yinshan and Ordos Blocks and redefined the belt as the Inner Mongolia Suture Zone (Kusky and Li 2003; Kusky et al. 2007). The Ordos block is mostly covered by Mesozoic to Cenozoic cover sequences and the metamorphic basement is inferred, based on geophysical data. The Yinshan block consists of the Neoarchean Wulashan Complex, Sertengshan Group and various orthogneisses which include tonalitic, granodioritic and dioritic gneisses, charnockites, hornblende adamellites, and hornblende granites, formed through the reworking of older (2.8–2.7 Ga) components (Geng et al. 2012).

A Neoarchean (2.8–2.5 Ga) accretion event (see Fig. 22.2) is recorded in the lower crustal xenoliths/xenocrysts from widely separated localities, such as the Paleozoic Mengyin and Fuxian kimberlites, the late Mesozoic Xinyang volcanic rocks, and the Cenozoic Pingquan, Hannuoba and Hebi basalts. This event coincides with a widespread crustal generation event seen in outcrop in the NCC (e.g., Jahn et al. 1988; Wu et al. 2005; Li and Kusky 2007; Jiang et al. 2010; Kusky 2011; Zhai 2011), and with a major global episode of crustal formation at ~2.7 Ga (Condie 2000; Zheng et al. 2004c, 2009b). The accretion also resulted in at least the local remelting of the ancient lower crust (i.e., in Xinyang). This Neoarchean lower crustal accretion event also may be recorded in the Re–Os model ages of the mantle peridotite xenoliths, such as in Hebi (Zheng et al. 2007; Liu et al. 2011) and in Fansi (Xu et al. 2008).

22.4.3 Paleoproterozoic (2.3–1.8 Ga) Reworking and Accretion of the Lower Crust

The Paleoproterozoic tectonothermal event is widely recorded in metasedimentary rocks, HP granulites, HP amphibolites, charnockites, S-type granites, and older gneisses in the NCC, especially in the Trans-North China Orogen, Khondalite Belt, and Jiao-Liao-Ji Belt (Fig. 22.1; Guan et al. 2002; Guo et al. 2002; Wan et al. 2005; Santosh et al. 2007; Zhao et al. 2010). A Paleoproterozoic U–Pb age peak was also found in zircons from the Phanerozoic sandstones (Yang et al. 2006) and modern clastic sedimentary rocks (Yang et al. 2009) within the NCC. Paleoproterozoic metamorphic zircon grains and thin overgrowth rims around old magmatic zircon cores are commonly found in the Fuping Complex (Zhao et al. 2000; Guan et al. 2002), Hengshan Complex (Wan et al. 2005) and in the Huai'an and Xuanhua Complexes (Guo et al. 2002), suggesting the main regional metamorphic event occurred at ~1.85 Ga (Zhao et al. 2000, 2010; Kusky 2011; Zhai 2011).

The Paleoproterozoic events also can be widely recognized in the lower crust beneath Fuxian, Yingxian, Xinyang, Junan, Hannuoba, and Nushan (Fig. 22.3). In Fuxian, some granulites contain abundant evidence for a significant thermal event at 1.8–1.9 Ga (Fig. 22.2a), and represent complete resetting of an older (2.7–2.5 Ga) population. However, in Yingxian (Fig. 22.2a), Xinyang (Fig. 22.2b) and Hannuoba (Fig. 22.2c) the event marked the addition of material derived from the asthenosphere. This event also produced widespread ~1.85 Ga S-type granites and associated basic rocks, and high-pressure mafic granulites of similar age (Zhao et al. 1999) in the NCC. At the eastern part of the southern edge of the NCC (i.e., Junan and Nushan), the Paleoproterozoic (2.3–2.2 Ga) events took place a little earlier than the collision between the EB and the WB (1.9–1.8 Ga) according to the suggestion of Zhao et al. (2000, 2010). They involved both the addition of magmas from the depleted mantle (Fig. 22.2b, c), and the reworking of the older (>3.0 Ga) crustal components. Therefore, the data from the lower crustal xenoliths are not adequate to distinguish between the competing models for the amalgamation of the NCC (Zhao et al. 2010; Kusky 2011) at this stage; further work will be required across a larger area.

22.4.4 Neoproterozoic (0.8–0.6 Ga) Reworking of the Lower Crust

The younger population of zircons in some Fuxian granulites appears to represent another episode of new zircon growth in the Neoproterozoic (Fig. 22.2a), indicating the breakdown of preexisting silicates and/or oxides to liberate Zr and radiogenic Hf. This event, poorly constrained at ca 600 Ma, does not correspond to any known major crustal event in the NCC. However, there is a widespread hiatus in sedimentation, represented by a regional disconformity across large parts of the craton, in Late Proterozoic to early Cambrian time (600–620 Ma; Piper and Zhang 1997). We suggest that this regional uplift reflects a thermal event (plume?) that affected (or reworked) the lower crust (Fig. 22.3), and is recorded in the younger zircons of some Fuxian mafic granulites (Zheng et al. 2004c).

22.4.5 Paleozoic—Early Mesozoic Reworking of the Lower Crust

Xenocrystic zircons from the Cenozoic Liaodong basalts (closed to the Paleozoic Fuxian kimberlites) in southern Liaoning Province have $\varepsilon_{Hf} = -16$, and reflect the reworking of the Archean basement in Paleozoic time (462 Ma; Zhang et al. 2011). This lower crustal reworking may correspond to the metasomatic event recorded in the Fuxian SCLM and the Fuxian kimberlitic activity (Lu et al. 1998). Other Paleozoic ages in lower crustal xenoliths/xenocrysts can be found in Xinyang (365 Ma in eclogite; Zheng et al. 2008) and Hannuoba (∼315 Ma in granulite xenoliths/xenocrysts; Zhang et al. 2012a).

The Xinyang and Hannuoba areas are at the southern and northern edges of the NCC, respectively, and also recorded the reworking of the lower crust during Paleozoic to early Mesozoic times. The Xinyang area is adjacent to the Qinling-Dabie-Sulu Orogenic Belt, formed by deep subduction and collision of the YC with the NCC in the early Paleozoic (∼440 Ma; Yang et al. 2005) and early Mesozoic time (220–240 Ma; Li et al. 1993). The Paleozoic collision is well recorded in the western part (i.e., the Qinling segment), and Mesozoic collision in the eastern part of the belt (i.e., the Dabie-Sulu segment). There are few data on the Tongbai segment adjacent to the Xinyang area; this is a region transitional between the Qinling and Dabie-Sulu belts. From the Xinyang area in the eclogite xenoliths 80 % of zircons give Paleozoic (377–263 Ma) U–Pb ages (Fig. 22.2b), recording strong modification of the lowermost crust of the southern margin of the NCC due to the subduction and collision of the Tongbai segment of the Qinling-Dabie-Sulu Orogenic Belt in late Paleozoic.

The Hannuoba area is adjacent to the southern edge of the eastern Central Asia Orogenic Belt. The belt, extending from Kazakhstan to the western Pacific Ocean, is a tectonic collage that separates the Siberian Craton to the north from the NCC and the Tarim block to the south. The major tectonic components of the fold belt include ophiolites, island arcs, oceanic islands, accretionary wedges, and some Precambrian microcontinents (Khain et al. 2003). Numerous geophysical and geochemical studies (Khain et al. 2003; Windley et al. 2007) document that this orogenic belt had a complicated history involving late Paleozoic subduction of oceanic crust, closure of paleo-oceans, and prolonged extensive magmatism, although the time of collision and tectonic style of the orogenic belt have been controversial for a long time. The subduction would be expected to modify the lithosphere along the northern edge of the NCC (e.g., Hannuoba).

22.4.6 Late Mesozoic–Cenozoic Accretion and Reworking

Zircons with ages of 120–45 Ma in the Hannuoba granulites, the Pingquan mafic granulites, and the xenocryst suite from Liaodong (Fig. 22.2c) may reflect thermal events accompanying basaltic underplating (addition) and the remelting (reworking) of the existing lower crust in late Mesozoic–Cenozoic time (Fig. 22.3). This underplating may be related to a stage of continental rifting which was a consequence of the dispersal of Gondwanaland, the accretion of Asia (Wilde et al. 2003), and the destruction of the NCC SCLM (Zheng et al. 2007; Zheng 2009). Following uplift and denudation, caused by compressional tectonics near the end of Cretaceous time, Paleogene continental rifting produced widespread continental margin basins in Eastern China (Ren et al. 2002).

Abundant zircons with ages of 45–47 Ma in the lower crustal xenoliths from Hannuoba may correspond to the thermal event accompanying this stage of continental rifting. All but two Paleogene zircon grains have positive ε_{Hf}. In contrast, the Mesozoic zircons have negative ε_{Hf} (Zheng et al. 2009a). This temporal variation in Hf isotopes may be relevant to the processes of crust–mantle interaction during the lithospheric thinning processes. In the early stages of the lithospheric thinning, either the underplating magmas were derived from an enriched lithospheric mantle, or the extent of crustal assimilation by the underplating magmas was larger than for those emplaced during later stages. Continuous magmatic underplating at Hannuoba (i.e., Paleogene) is basically consistent with the lithospheric thinning in the western NCC as inferred from basalt geochemistry (Xu et al. 2005), but contrasts with lithospheric thickening inferred in the eastern NCC during the Cenozoic (Zheng et al. 2009a).

Based on the discussion above, we conclude that the Xinyang area, at southern Henan Province of central China, is a very good place to summarize the processes of formation, reactivation, and destruction of continental craton. The oldest continental component ($\sim$4.0 Ga) of the NCC was found there. The locality lies on the southern margin of the NCC and the western margin of the EB of the craton (Fig. 22.1); it records abundant information on block–block interaction and thus mantle–crust interaction. The diatremes erupted at $\sim$160 Ma, an important conversion period in the tectonic framework, and carried a suite of xenoliths including lower crustal mafic to felsic granulites, eclogites, metagabbros, pyroxenites, and mantle peridotites (Zheng et al. 2003, 2004a, 2006). The petrological and geochemical data on the xenoliths show that the deep lithosphere in the area is temporally and compositionally zoned; exposed rocks up to ca 2.85 Ga old are underlain by felsic granulites and rare pyroxenites with zircon ages of 3.6–3.4 Ga (to ca 30 km depth) (Zheng et al. 2008). Deeper (ca 30–45 km) parts of the lower crust consist of high-pressure mafic to felsic granulites and metagabbros, which give Paleoproterozoic (2.0–1.8 Ga) zircon ages and show the significance of underplating and vertical crustal accretion (growth) in the Paleoproterozoic. The accretion was related to the amalgamation of the EB and WB of the craton (i.e., Zhao et al. 2010) and to the global assembly of the Columbia supercontinent (Kusky 2011) or cratonization (Zhai 2011). Hf-isotope data indicate that both juvenile material and remelting of older (3.8–3.0 Ga) crustal rocks were involved in this important event (Fig. 22.2b). Paleozoic (377–260 Ma) and early Mesozoic (228–219 Ma) zircons are also found in eclogites and peridotites, showing the gradual modification of the deeper part of the lower crust and the uppermost mantle due to the geodynamic processes related to the continental collision between this craton and the YC. Therefore, the deep-seated xenoliths from Xinyang diatremes record the growth and modification of the old (i.e., 4.0 Ga) continental lithosphere by magma underplating during several tectonic events (pre-late Mesozoic): assembly of the southern and northern parts of the EB in Neoarchean time, collision of the Western and Eastern Blocks in the possible Paleoproterozoic time, and subduction and collision of the YC with the NCC in the Paleozoic and the Triassic, respectively.

22.5 Conclusions

1. The North China Craton, one of the oldest (>3.65 Ga) cratons in the world, has been sampled by abundant xenolith-bearing Phanerozoic igneous rocks, making it an ideal area to study the formation and evolution of deep lithosphere. The oldest component of the craton is $\sim$4.0 Ga, which subsequently experienced complex accretion and reworking of the lower crust, and modification and replacement of the subcontinental lithospheric mantle.
2. The Neoarchean (2.8–2.5 Ga) and Paleoproterozoic (1.9–1.8 Ga) are two important growth periods of the North China Craton's lithosphere; a Neoproterozoic signal (0.6 Ga) can be locally found. Phanerozoic subduction of the Yangtze Craton affected the lowermost crust of the southern North China Craton. Accretion and modification of the lower crust beneath the craton are obvious along its northern margin during late Mesozoic–Paleogene time.
3. The North China Craton may have been more easily affected by subduction and collision with surrounding blocks, due to its small size compared to many other cratons worldwide. In early Mesozoic time, the subduction of the Yangtze Craton beneath the southern margin of the North China Craton may have resulted not only in a lateral spreading of the North China lithosphere, but also in mantle wedge metasomatism by fluids and/or melts derived from the subducted continental crust.

Acknowledgments This study was financially supported by the 973 project (2012CB416604), the National Natural Science Foundation of China (Grant Nos. 41130315, 91214204, 41520104003) and the MSF GPMR06.

References

Boyd, F. R. (1989). Compositional distinction between oceanic and cratonic lithosphere. *Earth and Planetary Science Letters, 96*(1–2), 15–26.

Chen, S. H., O'Reilly, S. Y., Zhou, X. H., Griffin, W. L., Zhang, G. H., Sun, M., et al. (2001). Thermal and petrological structure of the lithosphere beneath Hannuoba, Sino-Korean craton, China: Evidence from xenoliths. *Lithos, 56*(4), 267–301.

Chen, S. H., Zhang, G. H., Zhou, X. H., Sun, M., Feng, J. L., & Xie, Z. M. (1998). Petrological investigation on the Granulite Xenoliths from Hannuoba Basalts, Northern Sino-Korean Craton. *Acta Petrologica Sinica, 14*(3), 366–380. (in Chinese).

Condie, K. C. (2000). Episodic continental growth models: Afterthoughts and extensions. *Tectonophysics, 322*(1–2), 153–162.

Dobbs, P. N., Duncan, D. J., Hu, S., Shee, S. R., Colgan, E. A., Brown, M. A., et al. (1994). The geology of Mengyin kimberlites, Shandong, China. In O. A. Meyer & O. H. Leonardos (Eds.), *Kimberlites, related rocks and mantle xenoliths* (Vol. 1A/93, pp. 40–61). CPRM Special Publication.

Du, X. X., & Fan, Q. C. (2011). Discussion on genesis of pyroxenite and granulite xenoliths from Hannuoba. *Acta Petrologica Sinica, 27* (10), 2927–2936. (in Chinese).

Ernst, W. G., Tsujimori, T., Zhang, R. Y., & Liou, J. G. (2007). Permo-Triassic collision, subduction-zone metamorphism, and tectonic exhumation along the East Asian continental margin. *Annual Review of Earth and Planetary Sciences, 35*(1), 73–110.

Fan, Q. C., & Liu, R. X. (1996). The high-temperature high-pressure granulite xenoliths from Hannuoba basalts. *Chinese Science Bulletin, 41*(3), 235–238. (in Chinese).

Fan, Q. C., Liu, R. X., Li, H. M., Li, N., Sui, J. L., & Lin, Z. R. (1998). The zircon dating and REE of granulitic xenoliths from Hannuoba. *Chinese Science Bulletin, 43*(2), 133–137.

Fan, Q. C., Sui, J. L., Liu, R. X., & Zhou, X. M. (2001). Eclogite facies garnet-pyroxenolite xenolith in Hannnuoba area: New evidence of magma underplating. *Acta Petrologica Sinica, 17*(1), 1–6. (in Chinese).

Fan, Q. C., Zhang, H. F., Sui, J. L., Zhai, M. G., Sun, Q., & Li, N. (2005). Magma underplating and Hannuoba present crust-mantle transitional zone composition: Xenolith petrological and geochemical evidence. *Science China Earth Sciences, 48*(8), 1089–1105. (in Chinese).

Geng, Y. S., Du, L. L., & Ren, L. D. (2012). Growth and reworking of the early Precambrian continental crust in the North China Craton: Constraints from zircon Hf isotopes. *Gondwana Research, 21*(2-3), 517–529.

Guan, H., Sun, M., Wilde, S. A., Zhou, X. H., & Zhai, M. G. (2002). SHRIMP U-Pb zircon geochronology of the Fuping Complex: Implications for formation and assembly of the North China craton. *Precambrian Research, 113*(1–2), 1–18.

Guo, J. H., O'Brien, P. J., & Zhai, M. G. (2002). High-pressure granulites in the Sanggan area, North China craton: Metamorphic evolution, P-T paths and geotectonic significance. *Journal of Metamorphic Geology, 20*(8), 741–756.

Han, Q. J., & Shao, J. A. (2000). Mineral chemistry and metamorphic P-T conditions of granulite xenoliths in Early Mesozoic diorite in Harkin region, eastern Inner Mongolia autonomous region, China. *Earth Science, 25*(1), 21–27. (in Chinese).

Huang, X. L., Xu, Y. G., Chu, X. L., Zhang, H. X., & Liu, C. Q. (2001). Geochemical comparative studies of some granulite terranes and granulite xenoliths from North China Craton. *Acta Petrologica et Mineralogica, 20*(3), 318–328. (in Chinese).

Huang, X. L., Xu, Y. G., & Liu, D. Y. (2004). Geochronology, petrology and geochemistry of the granulite xenoliths from Nushan, east China: Implication for a heterogeneous lower crust beneath the Sino-Korean Craton. *Geochimica et Cosmochimica Acta, 68*(1), 127–149.

Huang, X. L., Xu, Y. G., Liu, D. Y., Jian, P. (2003). Paleoproterozoic lower crust beneath Nushan in Anhui Province: Evidence from zircon SHRIMP V-Pb dating on granulite xenoliths in Cenozoic alkali basalt. *Chinese Science Bulletin*, *48*(13), 1381–1385.

Jahn, B. M., Auvray, B., Shen, Q. H., Liu, D. Y., Zhang, Z. Q., Dong, Y. J., et al. (1988). Archean crustal evolution in China: The Taishan Complex and evidence for juvenile crustal addition from long-term depleted mantle. *Precambrian Research, 38*(4), 381–403.

Jiang, N., Carlson, R. W., & Guo, J. H. (2011). Source of Mesozoic intermediate-felsic igneous rocks in the North China Craton: Granulite xenolith evidence. *Lithos, 125*(1–2), 335–346.

Jiang, N., & Guo, J. H. (2010). Hannuoba intermediate-mafic granulite xenoliths revisited: Assessment of a Mesozoic underplating model. *Earth and Planetary Science Letters, 293*(3–4), 277–288.

Jiang, N., Guo, J. H., Zhai, M. G., & Zhang, S. Q. (2010). ~2.7 Ga crust growth in the North China Craton. *Precambrian Research, 179*(1–4), 37–49.

Khain, E. V., Bibikova, E. V., Salnikova, E. B., Kröner, A., Gibsher, A. S., Didenko, A. N., et al. (2003). The Palaeo-Asian ocean in the Neoproterozoic and early Palaeozoic: New geochronologic data and palaeotectonic reconstructions. *Precambrian Research, 122*(1-4), 329–358.

Kröner, A., Compston, W., Zhang, G., Guo, A., & Todt, W. (1988). Age and tectonic setting of late Archean greenstone-gneiss terrain in Henan Province, China, as revealed by single-grain zircon dating. *Geology, 16*(3), 211–215.

Kusky, T. M. (2011). Geophysical and geological tests of tectonic models of the North China Craton. *Gondwana Research, 20*(1), 26–35.

Kusky, T. M., & Li, J. H. (2003). Paleoproterozoic tectonic evolution of the North China Craton. *Journal of Asian Earth Sciences, 22*(4), 383–397.

Kusky, T., Li, J. H., & Santosh, M. (2007). The Paleoproterozoic North Hebei Orogen: North China Craton's collisional suture with the Columbia supercontinent. *Gondwana Research, 12*(1), 4–28.

Li, J. H., & Kusky, T. (2007). A Late Archean foreland fold and thrust belt in the North China Craton: Implications for early collisional tectonics. *Gondwana Research, 12*(1–2), 47–66.

Li, S. G., Xiao, T. L., Liou, D. L., Chen, Y. Z., Ge, N. J., Zhang, Z. Q., et al. (1993). Collision of the North China and Yangtze Blocks and formation of coesite-bearing eclogites: Timing and processes. *Chemical Geology, 109*(1–4), 89–111.

Liou, J. G., Hacker, B. R., & Zhang, R. Y. (2000). Into the forbidden zone. *Science, 287*(5456), 1215–1216.

Liu, D. Y., Nutman, A. P., Compston, W., Wu, J. S., & Shen, Q. H. (1992). Remnants of 3800 Ma crust in Chinese part of the Sino-Korean craton. *Geology, 20*(4), 339–342.

Liu, J. G., Rudnick, R. L., Walker, R. J., Gao, S., Wu, F. Y., Piccoli, P. M., et al. (2011). Mapping lithospheric boundaries using Os isotopes of mantle xenoliths: An example from the North China Craton. *Geochimica et Cosmochimica Acta, 75*(13), 3881–3902.

Liu, Y. S., Gao, S., Jin, S. Y., Hu, S. H., Sun, M., & Zhao, Z. B. (2001a). Geochemistry of lower crustal xenoliths from Neogene Hannuoba Basalt, North China Craton: Implications for petrogenesis and lower crustal composition. *Geochimica et Cosmochimica Acta, 65*(15), 2589–2604.

Liu, Y. S., Gao, S., Yuan, H. L., Zhou, L., Liu, X. M., Wang, X. C., et al. (2004). U-Pb zircon ages and Nd, Sr, and Pb isotopes of lower crustal xenoliths from North China Craton: Insights on evolution of lower continental crust. *Chemical Geology, 211*(1–2), 87–109.

Liu, Y. S., Gao, S., Zhou, L., Zhang, L., & Jin, S. Y. (2001b). Geochronology and geodynamic implications of the felsic granulite xenoliths from the Hannuoba Basalt. *Geochimica (Beijing), 30*(1), 51–56. (in Chinese).

Lu, F. X., Wang, Y., Chen, M. H., & Zheng, J. P. (1998). Geochemical characteristics and emplacement ages of the Mengyin kimberlites, Shandong Province, China. *International Geology Reveiw, 40*(11), 998–1006.

Menzies, M. A., Xu, Y. G., Zhang, H. F., & Fan, W. M. (2007). Integration of geology, geophysics and geochemistry: A key to understand the North China Craton. *Lithos, 96*(1), 1–21.

Peng, P., Zhai, M. G., Ernst, R. E., Guo, J. H., Liu, F., & Hu, B. (2008). A 1.78 Ga large igneous province in the North China craton: The Xiong'er Volcanic Province and the North China dyke swarm. *Lithos, 101*(3), 260–280.

Piper, J. D. A., & Zhang, Q. R. (1997). Palaeomagnetism of Neoproterozoic glacial rocks of the Huabei shield: The North China Block in Gondwana. *Tectonophysics, 283*(1), 145–171.

Polat, A., Li, J. H., Fryer, B., Kusky, T., Gagnon, J., & Zhang, S. (2006). Geochemical characteristics of the Neoarchean (2800–2700 Ma) Taishan greenstone belt, North China Craton: Evidence for plume-craton interaction. *Chemical Geology, 230*(1), 60–87.

Ren, J. Y., Tamaki, K., Li, S. T., & Zhang, J. X. (2002). Late Mesozoic and Cenozoic rifting and its dynamic setting in Eastern China and adjacent areas. *Tectonophysics, 344*(3), 175–205.

Santosh, M., Wilde, S. A., & Li, J. H. (2007). Timing of Paleoproterozoic ultrahigh-temperature metamorphism in the North China Craton: Evidence from SHRIMP U-Pb zircon geochronology. *Precambrian Research, 159*(3), 178–196.

Shao, J. A., Han, Q. J., & Li, H. M. (2000). Discovery of the Early Mesozoic granulite xenoliths in North China Craton. *Science in China, Series D: Earth Sciences, 43*(1), 245–252. (in Chinese).

Shao, J. A., & Wei, C. J. (2011). Petrology and tectonic significance of the Early Mesozoic granulite xenoliths from the eastern Inner Mongolia, China. *Science in China, Series D: Earth Sciences, 41*(8), 1080–1088. (in Chinese).

Shao, J. A., Zhang, Z., She, H. Q., & Liu, D. S. (2012). The discovery of Phanerozoic granulite in Chifeng area of North Craton and its implication. *Earth Science Frontiers*, *19*(3), 188–198 (in Chinese).

Song, B., Nutman, A. P., Liu, D. Y., & Wu, J. S. (1996). 3800 to 2500 Ma crustal evolution in the Anshan area of Liaoning Province, northeastern China. *Precambrian Research, 78*(1), 79–94.

Tang, H. Y., Zheng, J. P., Griffin, W. L., O'Reilly, S. Y., Yu, C. M., Pearson, N. J., et al. (2014). Complex evolution of the lower crust beneath the southeastern North China Craton: The Junan xenoliths and xenocrysts. *Lithos*, *206–207*, 113–126.

Wan, Y. S., Liu, D. Y., Song, B., Wu, J. S., Yang, C. H., Zhang, Z. Q., et al. (2005). Geochemical and Nd isotopic compositions of 3.8 Ga meta-quartz dioritic and trondhjemitic rocks from the Anshan area and their geological significance. *Journal of Asian Earth Sciences, 24*(5), 563–575.

Wei, Y., Zheng, J. P., Su, Y. P., Ma, Q., & Griffin, W. L. (2015). Lithological and age structure of the lower crust beneath the northern edge of the North China Craton: Xenolith evidence. *Lithos, 216–217*, 211–223.

Wilde, S. A., Zhou, X. H., Nemchin, A. A., & Sun, M. (2003). Mesozoic crust–mantle interaction beneath the North China craton: A consequence of the dispersal of Gondwanaland and accretion of Asia. *Geology, 31*(9), 817–820.

Windley, B. F., Alexeiev, D., Xiao, W., Kröner, A., & Badarch, G. (2007). Tectonic models for accretion of the Central Asian Orogenic Belt. *Journal of the Geological Society, 164*(1), 31.

Wu, F. Y., Zhao, G. C., Wilde, S. A., & Sun, D. Y. (2005). Nd isotopic constraints on crustal formation in the North China Craton. *Journal of Asian Earth Sciences, 24*(5), 523–545.

Wu, F. Y., Zhang, Y. B., Yang, J. H., Xie, L. W. & Yang, Y .H. (2008). Zircon U-Pb and Hf isotopic constraints on the Early Archean crustal evolution in Anshan of the North China Craton. *Precambrian Research*, *167*(3),339–362.

Xu, X. S., O'Reilly, S. Y., Griffin, W. L., & Zhou, X. M. (1998). The nature of the Cenozoic lithosphere at Nushan, eastern China. In M. Flower, S. L. Chung, & C. H. Lo (Eds.), *Mantle dynamics and plate internationals in East Asia* (Vol. 27, pp. 167–196). American Geophysical Union, Geodynamics Series.

Xu, Y. G., Blusztajn, J., Ma, J. L., Suzuki, K., Liu, J. F., & Hart, S. R. (2008). Late-Archaean to Early Proterozoic lithospheric mantle beneath the western North China craton Sr-Nd-Os isotopes of peridotite xenoliths from Yangyuan and Fansi. *Lithos, 102*(1), 25–42.

Xu, Y. G., Ma, J. L., Feigenson, M. D., Frey, F. A., & Liu, J. F. (2005). The role of lithosphere-asthenosphere interaction in the genesis of Quaternary tholeiitic and alkali basalts from Datong, western North China Craton. *Chemical Geology, 224*(4), 247–271.

Yang, J., Gao, S., Chen, C., Tang, Y. Y., Yuan, H. L., Gong, H. J., et al. (2009). Episodic crustal growth of North China as revealed by U-Pb age and Hf isotopes of detrital zircons from modern rivers. *Geochimica et Cosmochimica Acta, 73*(9), 2660–2673.

Yang, J. H., Wu, F. Y., Shao, J. A., Wilde, S. A., Xie, L. W., & Liu, X. M. (2006). Constraints on the timing of uplift of the Yanshan Fold and Thrust Belt, North China. *Earth and Planetary Science Letters, 246*(3), 336–352.

Yang, J. S., Liu, F. L., Wu, C. L., Xu, Z. Q., & Shi, R. D. (2005). Two ultrahigh-pressure metamorphic events recognized in the central orogenic belt of China: Evidence from the U-Pb dating of coesite-bearing zircons. *International Geology Review, 47*(4), 327–343.

Ye, K., Cong, B. L., & Ye, D. N. (2000). The possible subduction of continental materials to depths greater than 200 km. *Nature, 407*(6805), 334–336.

Ying, J. F., Zhang, H. F., Kita, N., Morishita, Y., & Shimoda, G. (2006). Nature and evolution of Late Cretaceous lithospheric mantle beneath the eastern North China Craton: Constraints from petrology and geochemistry of peridotitic xenoliths from Junan, Shandong Province, China. *Earth and Planetary Science Letters, 244*(3), 622–638.

Ying, J. F., Zhang, H. F., & Tang, Y. J. (2010). Lower crustal xenoliths from Junan, Shandong province and their bearing on the nature of the lower crust beneath the North China Craton. *Lithos, 119*(3), 363–376.

Yu, J. H., Xu, X. S., O'Reilly, S. Y., Griffin, W. L., & Zhang, M. (2003). Granulite xenoliths from Cenozoic Basalts in SE China provide geochemical fingerprints to distinguish lower crust terranes from the North and South China tectonic blocks. *Lithos, 67*(1), 77–102.

Zhai, M. G. (2011). Cratonization and the Ancient North China Continent: A summary and review. *Science China-Earth Sciens, 54*(8), 1110–1120.

Zhai, M. G., Fan, Q. C., & Zhang, H. F. (2007). Lower crustal processes leading to Mesozoic lithospheric thinning beneath eastern North China: Underplating, replacement and delamination. *Lithos, 96*(1), 36–54.

Zhai, M. G., Guo, J. H., & Liu, W. J. (2001). An exposed cross-section of early Precambrian continental lower crust in North China craton. *Physics and Chemistry of the Earth (A), 26*(9), 781–792.

Zhang, G. H., Zhou, X. H., Sun, M., Chen, S. H., & Feng, J. L. (1998). Highly chemical heterogeneity in the lower crust and crust-mantle transitional zone: geochemical evidences from xenoliths in Hannuoba basalt, Hebei Province. *Geochimica, 27*(2), 153–169. (in Chinese).

Zhang, H. F. (2012). Destruction of ancient lower crust through magma underplating beneath Jiaodong Peninsula, North China Craton: U-Pb and Hf isotopic evidence from granulite xenoliths. *Gondwana Research, 21*(1), 281–292.

Zhang, H. F., Yang, Y. H., Santosh, M., Zhao, X. M., Ying, J. F., & Xiao, Y. (2012a). Evolution of the Archean and Paleoproterozoic lower crust beneath the Trans-North China Orogen and the Western Block of the North China Craton. *Gondwana Research, 22*(1), 73–85.

Zhang, H. F., Ying, J. F., Tang, Y. J., Li, X. H., Feng, C., & Santosh, M. (2011). Phanerozoic reactivation of the Archean North China Craton through episodic magmatism: Evidence from zircon U-Pb geochronology and Hf isotopes from the Liaodong Peninsula. *Gondwana Research, 19*(2), 446–459.

Zhang, H. F., & Zheng, J. P. (2003). Geochemical characteristics and petrogenesis of Mesozoic basalts from the North China Craton: A Case Study in Fuxin, Liaoning Province. *Chinese Science Bulletin, 48*(9), 924–930.

Zhang, J., Zhang, H. F., Ying, J. F., Tang, Y. J., & Niu, L. F. (2008). Contribution of subducted Pacific slab to Late Cretaceous mafic magmatism in Qingdao region, China: A petrological record. *Island Arc, 17*(2), 231–241.

Zhang, S. H., Zhao, Y., & Santosh, M. (2012b). Mid-Mesoproterozoic bimodal magmatic rocks in the northern North China Craton: Implications for magmatism related to breakup of the Columbia supercontinent. *Precambrian Research, 222–223*, 339–367.

Zhao, G. C., Cawood, P. A., Wilde, S. A., Sun, M., & Lu, L. Z. (2000). Metamorphism of basement rocks in the Central Zone of the North China Craton: Implications for Paleoproterozoic tectonic evolution. *Precambrian Research, 103*(1), 55–88.

Zhao, G. C., Wilde, S. A., Cawood, P. A., & Lu, L. Z. (1999). Thermal evolution of two textural types of mafic granulites in the North China craton: Evidence for both mantle plume and collisional tectonics. *Geological Magazine, 136*(3), 223–240.

Zhao, G. C., Wilde, S. A., Guo, J. H., Cawood, P. A., Sun, M., & Li, X. P. (2010). Single zircon grains record two Paleoproterozoic collisional events in the North China Craton. *Precambrian Research, 177*(3), 266–276.

Zheng, J. P. (2009). Comparison of mantle-derived materials from different spatiotemporal settings: Implications for destructive and accretional processes of the North China Craton. *Chinese Science Bulletin, 54*(19), 3397–3416.

Zheng, J. P., Griffin, W. L., O'Reilly, S. Y., Hu, B. Q., Zhang, M., Pearson, N., et al. (2008). Continental collision/accretion and modification recorded in the deep lithosphere of central China. *Earth Planetary Science Letters, 269*(3), 496–506.

Zheng, J. P., Griffin, W. L., O'Reilly, S. Y., & Lu, F. X. (2004a). 3.6 Ga lower crust in central China: New evidence on the assembly of the North China Craton. *Geology, 32*(3), 229–232.

Zheng, J. P., Griffin, W. L., O'Reilly, S. Y., Lu, F. X., & Yu, C. M. (2004b). U-Pb and Hf-isotope analysis of zircons in mafic xenoliths from Fuxian kimberlites: Evolution of the lower crust beneath the North China Craton. *Contributions to Mineralogy and Petrology, 148*(1), 79–103.

Zheng, J. P., Griffin, W. L., O'Reilly, S. Y., Yu, C. M., Zhang, H. F., Pearson, N., et al. (2007). Mechanism and timing of lithospheric modification and replacement beneath the eastern North China Craton: Peridotitic xenoliths from the 100 Ma Fuxin basalts and a regional synthesis. *Geochimica et Cosmochimica Acta, 71*(21), 5203–5225.

Zheng, J. P., Griffin, W. L., O'Reilly, S. Y., Zhang, M., & Pearson, N. (2006). Zircons in mantle xenoliths record the Triassic Yangtze—North China continental collision. *Earth Planetary Science Letters, 247*(1), 130–142.

Zheng, J. P., Griffin, W. L., O'Reilly, S. Y., Zhao, J. H., Wu, Y. B., Liu, G. L., et al. (2009a). Neoarchean (2.7–2.8 Ga) accretion beneath the North China Craton: U-Pb age, trace elements and Hf isotopes of zircons in diamondiferous kimberlites. *Lithos, 112*(3), 188–202.

Zheng, J. P., Griffin, W. L., Ma, Q., O'Reilly, S. Y., Xiong, Q., Tang, H. Y., et al. (2012). Accretion and reworking beneath the North China Craton. *Lithos, 149*, 61–78.

Zheng, J. P., Griffin, W. L., Qi, L., O'Reilly, S. Y., Sun, M., Zheng, S., et al. (2009b). Age and composition of granulite and pyroxenite xenoliths in Hannuoba basalts reflect Paleogene underplating beneath the North China Craton. *Chemical Geology, 264*(1), 266–280.

Zheng, J. P., Lu, F. X., & Yu, C. M. (2004c). An in situ zircon Hf isotopic, U-Pb age and trace element study of banded granulite xenoliths from Hannuoba basalt: Tracking the early evolution of the lower crust in the North China Craton. *Chinese Science Bulletin, 49*(3), 277–285.

Zheng, J. P., Sun, M., & Lu, F. X. (2003). Mesozoic lower crustal xenoliths and their significance in lithospheric evolution beneath the Sino-Korean Craton. *Tectonophysics, 361*(1), 37–60.

Zheng, J. P., Zhang, R. S., Yu, C. M., Tang, H. Y., & Zhang, P. (2004d). In situ zircon Hf isotopic, U-Pb age and trace element study of monzonite xenoliths from Pingquan and Fuxin basalts: Tracking the thermal events of 169 Ma and 107 Ma in Yanliao area. *Science in China (Ser. D)*, *47*(z2), 39–52.

Zhou, X. H., Sun, M., Zhang, G. H., & Chen, S. H. (2002). Continental crust and lithospheric mantle interaction beneath North China: Isotopic evidence from granulite xenoliths in Hannuoba, Sino-Korean craton. *Lithos, 62*(3), 111–124.

Zhou, X. M., Yu, J. H., & Xu, X. S. (1992). Discovery and significance of granulite xenoliths in the Nushan basalt, East China. *Chinese Science Bulletin, 37*(20), 1730–1734.

Zhu, R. X., Chen, L., Wu, F. Y., & Liu, J. L. (2011). Timing, scale and mechanism of the destruction of the North China Craton. *Science China Earth Sciences, 54*(6), 789–797. (in Chinese).